Tribol Lett
DOI 10.1007/s11249-011-9750-5

ORIGINAL PAPER

The Roles of Statics and Dynamics in Determining Transitions Between Atomic Friction Regimes

Yalin Dong · Danny Perez · Arthur F. Voter · Ashlie Martini

Received: 29 September 2010 / Accepted: 7 January 2011

Abstract We introduce a model AFM tip/substrate system that includes full atomistic detail as well as system compliance to study the transitions between three regimes of atomic friction: smooth sliding, stick-single slip, and stick-multiple slip. We characterize these atomic friction regimes in terms of static and dynamic effects, and investigate how the slip modes affect the mean friction. Molecular statics calculations show that reduced-order model predictions of possible transitions between slip regimes are generally adequate for a fully atomistic system, even for complex reaction coordinates. However, molecular dynamics simulations demonstrate that, while static features of the system govern possible slip regimes, dynamic effects ultimately determine actual transitions between slip regimes.

Keywords Nanotribology · Stick-slip · Dynamic modeling · Friction mechanisms

1 Introduction

Finding ways to control friction at an atomic level has become an area of extreme interest with the development of micro- and nano-scale mechanical components [1–4]. For this purpose, atomic-scale friction has been widely studied using the Atomic/Friction Force Microscope (AFM/FFM), as well as molecular dynamics (MD) simulations and reduced-order modeling. The first measurements of atomic stick slip friction were obtained by Mate et al. using a tungsten tip sliding against graphite [5]. An interpretation of the underlying mechanisms was subsequently described by Tománek et al. [6]. A simplified model of the experimental system can be described as follows: the AFM tip is confined in the potential energy corrugation of the substrate surface and is connected to a support by an elastic cantilever. When the support is moved laterally, the tip is gradually pulled out from its current potential energy well and into the next one. During this process, the friction is measured by monitoring the deflection of the cantilever.

Depending on the conditions, atomic-scale friction can be observed in three distinct regimes: smooth sliding, where the tip moves continuously; stick-single slip, where the tip repeatedly sticks and then jumps forward a distance of one lattice spacing; and stick-multiple slip, where the jumps span multiple lattice spacings. These regimes differ not only in their atomic scale mechanisms but also the frictional behavior they are associated with. For example, the instability of stick-slip typically causes the resulting mean friction to be quite high, while in the absence of stick-slip, the two surfaces slide smoothly relative to each other, which can lead to ultralow friction [2, 4].

Transitions between atomic friction regimes are linked to changes in the topology of the potential energy landscape on which the system evolves. More specifically, the maximal length of a slip is related to the number of local energy minima accessible at any given time. For example, if the potential energy landscape contains a single minimum at any position of the cantilever, slip cannot occur and smooth sliding is observed. Similarly, if two (n) minima are available, then single (n-1-fold) slips are in

Y. Dong · A. Martini (✉)
Purdue University, West Lafayette, IN, USA
e-mail: a-martini@purdue.edu

D. Perez · A. F. Voter
Theoretical Division T-1, Los Alamos National Laboratory, Los Alamos, NM, USA

Published online: 29 January 2011

principle possible. By relying on the 1D single-spring Tomlinson Hamiltonian to describe the energetics of the system—whereby the tip and cantilever are coarse-grained into a single spring of stiffness K_{eff} and the corrugation is introduced through a one-dimensional sinusoidal potential of amplitude E_0 and period a—Medyanik et al. showed [7] that the onset of different regimes could be predicted using a single parameter, η. For the Hamilonian described above, the critical values $\eta = 1$, 4.6, 7.79, and 10.95 are associated with transitions to single, double, triple, and quadruple slips, respectively. While the simplicity of this model—henceforth referred to as the MLSC model (first letters of the authors' last names)—is appealing, the robustness of these critical values against the specific form of the simplified Hamiltonian in the general case, where the reaction coordinate for slip might be complex and embedded within a high-dimensional space, has not been assessed. Indeed, while it was recently shown that, *close to instability points*, the effective Hamiltonian associated with a commensurate Cu on Cu interface is well approximated by a Tomlinson Hamiltonian [8], the global representativeness of this form, especially for more general, incommensurate interfaces, has still not been established.

Both modeling and experiment have shown that there are transitions between atomic friction regimes, and that the occurrence of these transitions is dependent on the static and dynamic characteristics of a system [1, 7, 9, 10]. However, reduced order models and experimental measurements usually do not provide information about the atomic-level details underlying these transitions. These limitations suggest the use of fully atomistic calculations and simulations. These techniques have the advantage that, unlike simple theories, they rely only weakly on idealized assumptions (unlike model Hamiltonians) and consequently can take the detailed characteristics of the system into consideration. They also provide a complete resolution in both space and time from which, unlike experimental methods currently available, one can extract unambiguous atomic-level explanations for observed phenomena and assess theoretical predictions. It is also well known that dynamical factors such as temperature, sliding velocity [11–15], and damping [16, 17] can profoundly affect observed frictional behavior. These factors, which are unaccounted for in a static analysis like that of MLSC, can be studied directly using a fully atomistic approach.

In this article, we report a numerical investigation of the different friction regimes using fully atomistic models, both molecular dynamics (MD) simulation and molecular statics (MS) calculations. We investigate how the atomistic properties of the interface and the compliance of the system affect friction and we assess the validity of the MLSC model by explicitly identifying the transition points between smooth sliding, stick-single slip, and stick-multiple slip. We then characterize atomic friction regimes in terms of static—compliance, interface commensurability—and dynamic—temperature, scanning velocity—effects, and investigate how the slip modes affect the mean friction.

2 Methodology

Anticipating potential comparison with experiments in the future, we choose platinum as the model tip material, gold as the substrate, and a (111) sliding surface. These choices are made because the platinum (111) and gold (111) surfaces have low surface energy so that welding at the interface will be limited. Both platinum and gold atoms are modeled by the embedded atom method (EAM) potentials of Voter–Chen form [18]. For gold–platinum interactions, the EAM electronic density function is re-scaled so that the summed electron densities match for face centered cubic Pt and Au, and an arithmetic mean of the pure material pair potentials is applied to create the cross pair potential between gold and platinum.

The Pt/Au tip/substrate model shown in Fig. 1 is similar to that we have reported before for a Cu/Cu system [19]. In this study, however, we introduce virtual atoms to incorporate the cantilever compliance. Virtual atoms (red shells in Fig. 1) have the mass of a Pt atom but do not experience or contribute to EAM interactions; they are instead coupled to individual Pt atoms in the top three layers of the tip through a harmonic potential with spring constant K_i. The effective cantilever stiffness is then $K_l = \sum K_i$. Consistent

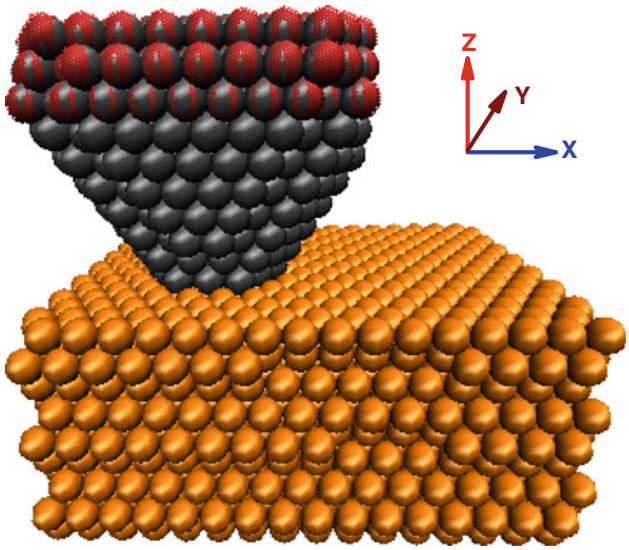

Fig. 1 Illustration of the model system where platinum tip atoms are shown in *gray* and *gold* substrate atoms in *yellow*. The *red* shells are virtual atoms which are coupled one by one to the atoms in the upper layers of the tip by harmonic springs. See text for detail (Color figure online)

with physical AFM experiments, the three cartesian components of spring stiffness are allowed to differ from one another. In the simulation, the stiffness of springs in the direction normal to the surface (z) is kept constant, while it is varied in the other two directions (x and y). This ensures that unphysically large tilts of the tip will not occur when soft (i.e., very compliant) cantilevers are considered.

During the simulation, the virtual atoms (collectively referred to as the support) are uniformly translated at a constant scanning velocity in the x ($\langle\bar{1}01\rangle$) direction. They are further restricted from any movement in the y direction, but allowed to move in z as a rigid body so as to enforce a desired external load (0 N/m in this case). The tip is then driven laterally through interactions between the real atoms and the virtual atoms. The only other constraint on the system is that the bottommost three layers of atoms in the substrate are fixed. Temperature is controlled by applying a Langevin thermostat to the atoms four layers away from the tip–substrate interface. Dynamical simulations were run using standard MD and parallel replica dynamics (Par-Rep). Par-Rep is an accelerated MD method through which simulations replicas are run parallel in time to extend their total duration, thereby enabling lower sliding speeds [19, 20]. Simulations with velocities of 0.1 m/s or less were run using Par-Rep; above this speed simulations were performed using standard MD. Molecular statics (MS) calculations [8] were performed using the L-BFGS minimization algorithm [21] and transition pathways were identified using the string method [22].

The transition parameter derived from the MLSC model is defined as $\eta = 2\pi^2 E_0/K_{\text{eff}}a^2$ where E_0 and a are the amplitude and periodicity of the potential energy corrugation, respectively, and K_{eff} is the effective spring stiffness. These parameters are obtained for our system as follows. First, sequences of MS calculations are carried out to identify all the mechanically stable states available to the contact as the support is translated by a. From this data, the effective stiffness of the system is characterized in terms of two contributions: that of the cantilever and of the main body of the tip K_{l} (as modeled by the springs between virtual and real atoms), and that of the apex of the tip K_{t}. By measuring the forces acting on the virtual atoms as well as the corresponding deflections of the tip, we infer $K_{\text{t}} = 56.8$ N/m for our setup. By combining these two values, the effective stiffness becomes:

$$\frac{1}{K_{\text{eff}}} = \frac{1}{K_{\text{t}}} + \frac{1}{K_{\text{l}}}. \quad (1)$$

The amplitude of the effective potential energy corrugation is extracted from these calculations using one of two methods. In cases where a single family of potential energy minima is present, the corrugation is mapped by directly computing the interaction energy between the tip and the surface. In cases where more than one minimum is available, the transition (minimum energy) pathways between the different minima are computed explicitly with the string method and the potential energy corrugation inferred from the tip/surface interaction energy along the pathways.

Due to the time- and length-scale limitations inherent to atomistic simulations, our model only explicitly considers the apex of the tip, while the compliance of the body of the tip and of the cantilever are included in an effective fashion through the interaction between real and virtual atoms. This coarse-graining process is energetically sound and captures the dynamics of the fast apex modes [23, 24]. It however dramatically underestimates the inertia associated with the motion of the cantilever, which can in turn underestimate the duration of slips events, particularly for soft cantilevers. These limitations are currently being relaxed and their impact on the slip dynamics will be reported elsewhere.

3 Results and Discussion

3.1 System Compliance

MS calculations were used to investigate the effect of compliance on atomic stick-slip friction. The cantilever stiffness K_{l} was varied between 25 to 2,500 N/m so as to cover most of the experimentally relevant range (Bennewitz et al. report $K_{\text{l}} = 16.5$ and 4,475 N/m [25], Carpick et al., $K_{\text{l}} = 190$ N/m [26], and Lantz et al. $K_{\text{l}} = 110$ and

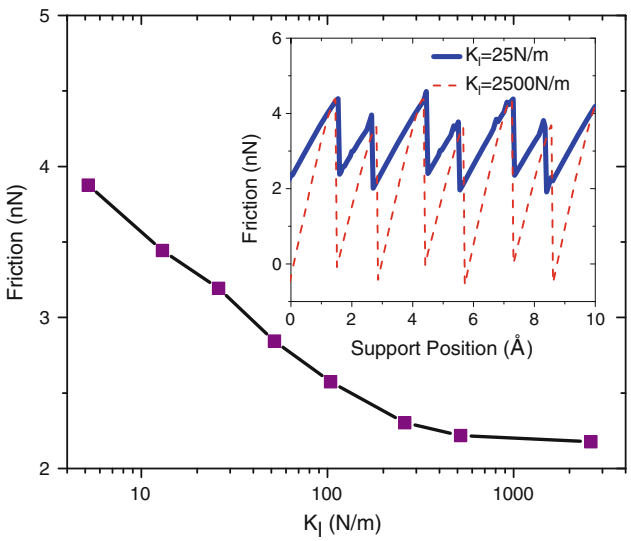

Fig. 2 Compliance dependence of mean friction force for the commensurate interface. *Inset* representative friction traces from simulations with cantilever stiffness varying by two orders of magnitude

8.1 N/m [27]). The impact of K_l on the friction force is summarized in Fig. 2. The results show that the mean friction decreases significantly with increasing cantilever stiffness as has been noted before [28, 29]. We also observe that, as the cantilever stiffness increases (i.e., the cantilever becomes less compliant), the mean friction approaches a limiting value. This is expected given that Eq. 1 converges to K_t as $K_l \rightarrow \infty$.

3.2 Stick-Slip and Smooth Sliding

As discussed above, smooth sliding should prevail whenever the effective stiffness of the system is so large that a single configuration of the contact is stable at any support position. According to the MLSC model, this should occur when K_{eff} is such that η is less than 1. We use MS calculations to predict friction for systems with a wide range of compliance as shown in Fig. 2 and observed distinct stick-slip in all cases. For our model system, the smallest value of the transition parameter, $\eta = 4.37$ (where $E_0 = 1.63$ eV and $K_l = 2{,}500$ N/m), is significantly larger than 1, which is consistent with our observation of stick-slip. This illustrates that it is not always possible to achieve smooth sliding by increasing the cantilever stiffness alone since the finite intrinsic stiffness of the tip's apex might prevent the elastic energy from completely overcoming the interfacial energy corrugation.

The results shown thus far have been obtained from a commensurate contact where the tip and surface are initially in Face Centered Cubic (FCC) registry (the similarity of the Au and Pu lattice constants allows them to behave quasi-commensurably for small enough contact areas). In practice the interface is likely to be incommensurate because of angular misalignment between the two interfaces, and it has been shown that the incommensurability of the tip and the substrate will affect surface energy corrugation [1, 30] and therefore friction. We find this to be the case for our Au/Pt system as well. As shown in Fig. 3 for a stiff cantilever ($K_l = 2{,}500$ N/m), changing the orientation of the tip relative to the substrate can significantly affect friction: changing the relative mismatch angle from 0° to 30° results in both a decrease of mean friction from 2.18 nN to almost 0 as well as a transition from stick-slip to smooth sliding. This transition is evident in Fig. 3 as the contrast between the smooth friction trace and displacement of the incommensurate case (30°) and the distinct force drops and displacement jumps of the commensurate case (0°).

By mapping the potential energy landscape of the system as a function of the stiffness using MS, we predict that the transition to smooth sliding, signaled by the observation of a single continuous family of minima, should occur around $K_l = 411$ N/m ($K_{eff} = 49.4$ N/m). The signature of this transition can be extremely subtle as the force discontinuity is initially vanishingly small. As shown in the inset of Fig. 4, the force trace at $K_l = 411$ N/m bears no obvious sign of stick-slip. Only with $K_l = 20$ N/m or smaller can one observe the characteristic saw-tooth pattern. The period and amplitude of the potential energy corrugation at the critical stiffness case are 2.88 Å and 1.08 eV, respectively, such that the MS-predicted MLSC parameter corresponds to $\eta = 0.83$, in reasonable agreement with the theoretical

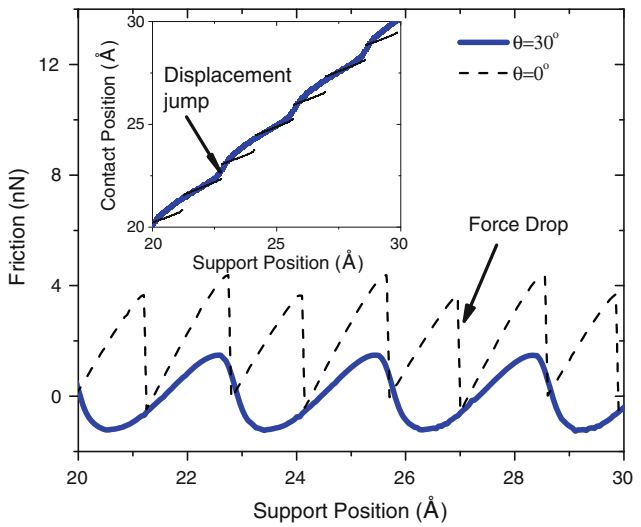

Fig. 3 Friction traces at tip-sample rotation angles of $\theta = 0°$ and 30° for $K_l = 2{,}500$ N/m illustrating the effect of commensurability on mean friction and the transition between smooth sliding and stick-slip. The *inset* shows the displacement of the tip contact atoms as a function of support position for the two cases

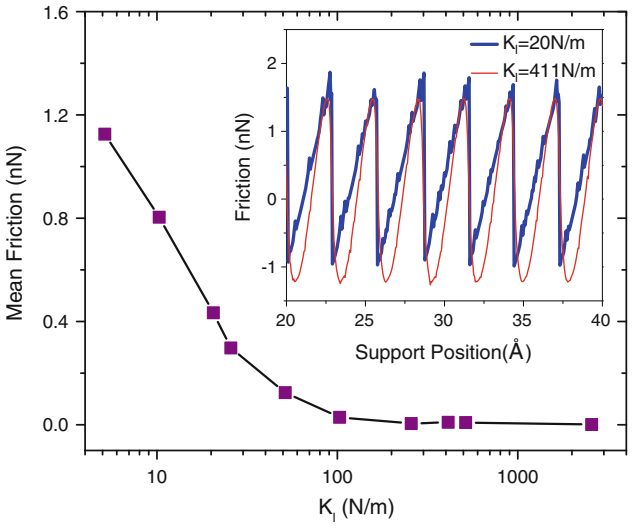

Fig. 4 Friction as a function of cantilever compliance in incommensurate contact ($\theta = 30°$). *Inset* force traces corresponding to different cantilever compliances. The cantilever compliance at which the transition from smooth sliding to stick-slip predicted by MS calculation is $K_l = 411$ N/m

prediction ($\eta = 1$). This shows that, despite the complex, incommensurate, structure of the interface and the angular mismatch, the effective Hamiltonian along the reaction coordinate is well approximated by a simple Tomlinson form.

Formally speaking, the transition from smooth sliding to stick-slip cannot be postponed by dynamical effects. Indeed, in the stick-slip regime, there is no continuous path available for the system to evolve along and slip to a disjoint family of energy minima will necessarily occur at some point; conversely, in the smooth sliding regime, there is no other family of minima to slip to. The subtle force signature of this transition is demonstrated in Fig. 4, where the variation of the mean friction with cantilever compliances is reported for the incommensurate system ($\theta = 30°$). The results show that the decay of the mean friction force with increasing stiffness is very smooth and gradual. Furthermore, at the critical stiffness, the force trace bears no obvious sign of stick-slip (c.f. inset of Fig. 4); only the superposition of two distinct families of minima for an extremely narrow band of support positions near the maxima of the friction force reveals that smooth sliding can no longer occur.

Thus, our results are consistent with the expectation that the transition between smooth sliding and stick-slip is dependent on both cantilever stiffness and orientation. For commensurate surfaces, the system exhibits stick-slip regardless of cantilever compliance, but the mean friction associated with that stick-slip decreases with increasing stiffness (from 4 to 2.18 nN). Introducing incommensurability into the system enables it to attain smooth sliding with an ultralow friction. These results agree with the predictions of the MLSC model.

3.3 Single and Multiple Slip

As the stiffness of the cantilever decreases, the energy landscape on which the system evolves becomes increasingly dominated by contributions from the interfacial energy corrugation. This causes an increase in the number of mechanically stable states that the contact can occupy. When this number is larger than 2, multiple slips, i.e., rapid sequences of correlated slips, become possible. Since the occurrence of long slips can affect friction, it is of interest to understand the transition between these different regimes.

In the framework of the MLSC model, transitions are controlled by the η parameter as discussed previously. Again, this model is based on the assumption that the elastic and corrugation energies are quadratic and sinusoidal, respectively, along the same one-dimensional coordinate. However, when the transition coordinate for slip is not co-linear with the scanning direction, this hypothesis is likely to be violated. For example, our atomistic model reveals that, instead of moving along a straight line parallel to the scanning direction, the commensurate contact moves following a zigzag pattern corresponding to transitions from FCC to HCP (Hexagonal Close-Packed) sites, and then from HCP to FCC sites. The transition between FCC and HCP, apparent in Fig. 2, has also been observed in a Cu/Cu system [8, 31]. This is also the reason why the period of the force trace for incommensurate contact is twice that of commensurate contact as shown in Fig. 3.

To investigate the impact of this complex reaction coordinate, we gradually decreased the cantilever stiffness acting on the commensurate contact and scanned the support position with MS until the number of minima available at any support position changed from 2 to 3 (indicating the possible onset of double slips) and from 3 to 4 (indicating the possible outset of triple slips). Using this procedure, we determined that the transition points were approximately $K_l = 1{,}028$ and 61.5 N/m, respectively. The effective energy landscapes corresponding to these two transition points for a fixed support position x_s, taken in the very narrow range where a maximal number of minima are simultaneously present, are shown in Fig. 5. Indeed, at a critical value of the stiffness, the number of accessible minima will increase by one only for a single value of x_s. Consequently, minima at the ends of the corresponding pathways will initially be very shallow, as shown in Fig. 5. It can be seen that three minima (indicated by dashed arrows in Fig. 5) are indeed present along the energy pathways for $K_l = 1{,}028$ N/m and that four of them are

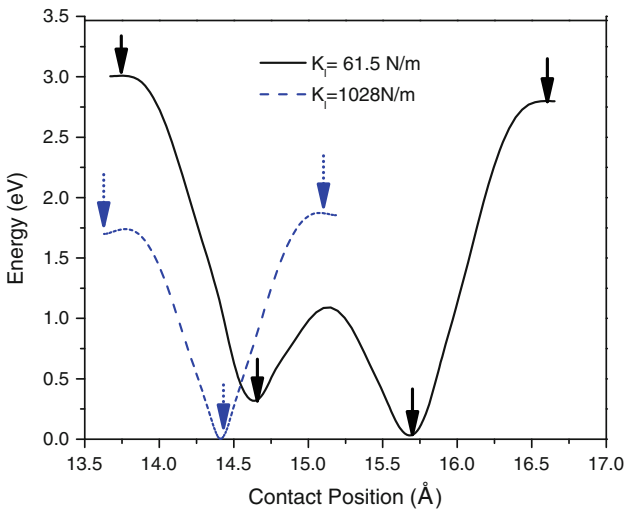

Fig. 5 Minimum energy pathways connecting different mechanically stable states for a fixed support position x_s where a maximal number of minima coexist. The minima are identified by *arrows*. *Dashed curve*: transition from single to possible double slips: $K_l = 1,028$ N/m, $x_s = 14.05$ Å; *Solid curve*: transition from possible double to possible triple slips: $K_l = 61.5$ N/m, $x_s = 14.85$ Å

present at $K_1 = 61.5$ N/m. The transition parameters for these two conditions are $\eta = 4.56$ and 8.64 (given $E_0 = 1.7$ eV), which is again in reasonable agreement with the values predicted by MLSC model, $\eta = 4.60$ and 7.79, respectively.

The modest discrepancy can be explained in terms of the inadequacy of a 1D coordinate to fully represent the energetics in this case. As shown in Fig. 6, while the corrugation energy is adequately approximated by a sinusoidal function with respect to the displacement of the contact along the scanning direction, the elastic energy deviates from simple quadratic behavior. This is caused by the fact that the contact also moves perpendicularly to the scanning direction as it slips between FCC and HCP sites. In this case the result is that the MLSC model underestimates the true elastic energy, leading to a modest error in the prediction of the critical stiffness. However, given that most of the displacement still occurs along the 1D coordinate, the correction is mild; in more general cases however, significant deviations cannot be excluded.

In contrast with the transition from smooth sliding to single stick-slip, this analysis provides only a statement of the possibility of multiple slips of a given length. In reality, dynamical considerations are crucial to determine the actual slip length. Indeed, some minima are only accessible over an extremely small range of support positions (formally infinitesimally small at the stiffnesses where the number of overlapping minima changes). Further, the fact that these states exist does not ensure that they are dynamically accessible as significant energy barriers (potentially many eV high) might separate them (c.f., Fig. 5). The actual occurrence of multiple slips thus requires that sufficient elastic energy be released during slips, that this energy is sufficient to activate the crossing of the barriers separating the different minima, and that it is not dissipated before the next slip can occur. Note that, because of its intrinsically dynamical (in contrast to thermodynamical) nature, the physics of multiple correlated slips is typically absent from rate-theory based models [8, 11, 12]. Direct numerical simulation is therefore currently the most practical way to access this information reliably.

In order to understand the importance of these dynamical factors, we use MD to simulate stick-slip friction with a very soft cantilever where a large number of states are available to the system. Because computational limitations prohibit us from taking the considerable inertia of the cantilever into account in the model, the timescale over which slips occur (μs to ms in typical experimental conditions [32]) will be severely underestimated. To compensate, we apply a correspondingly large Langevin damping coefficient (close to critical with respect to the slowest vibrational modes) to the topmost atoms of the tip. Because it is not possible to rigorously map these conditions back to experimental ones, the following results cannot be expected to provide quantitative predictions. However, given the generic nature of our fully atomistic model, our MD simulation are expected to provide qualitatively correct insights for the dynamical factors affecting multiple slips. Note that 1D models are particularly sensitive to the value of the damping parameter because this parameter alone controls the flux of energy in and out of the reaction coordinate. In contrast, due to its high-dimensional nature and the corresponding availability of a large number of other modes to couple to, our atomistic

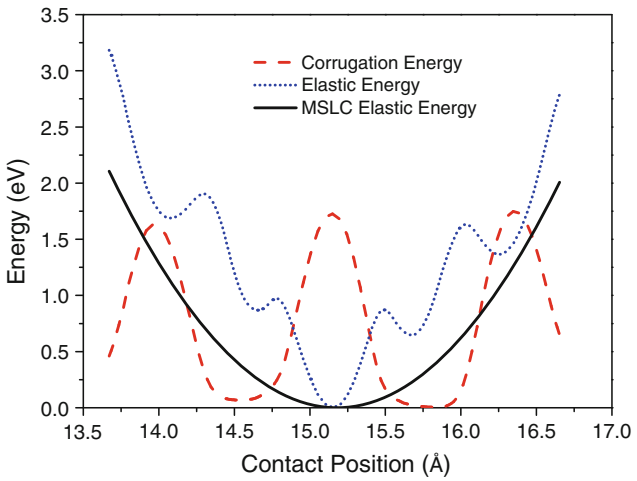

Fig. 6 Corrugation (*dashed red line*) and elastic (*dotted blue line*) energy contributions along the minimum energy pathway for $K_1 = 61.5$ N/m and $x_s = 14.85$ Å. The MLSC-predicted elastic energy (*solid black line*) is shown for comparison (Color figure online)

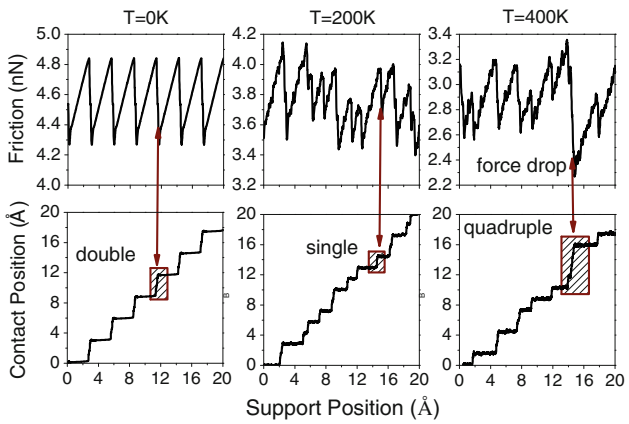

Fig. 7 The effect of temperature on multiple-slip: friction force (*top*) and corresponding contact position (*bottom*), as functions of support position for temperatures of 0, 200, and 400 K. Larger jump lengths of the contact position at higher temperatures indicate more multiple-slips

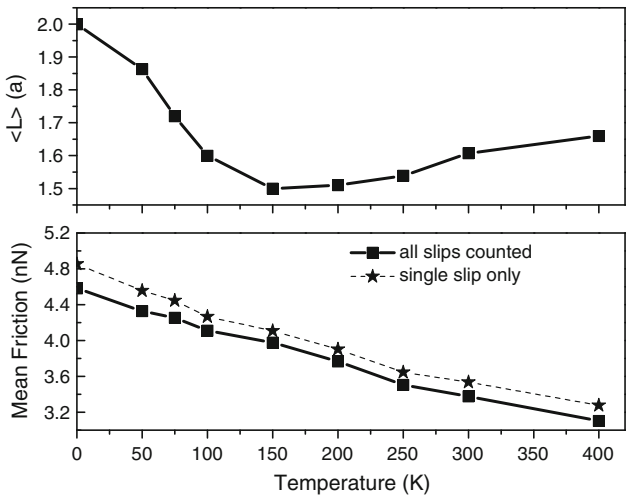

Fig. 8 Average slip length $\langle L \rangle$ and mean friction as a function of temperature. The *solid line* is the measured average and the *dash line* is the predicted average if only single slips would have occurred. a is the length of a single slip

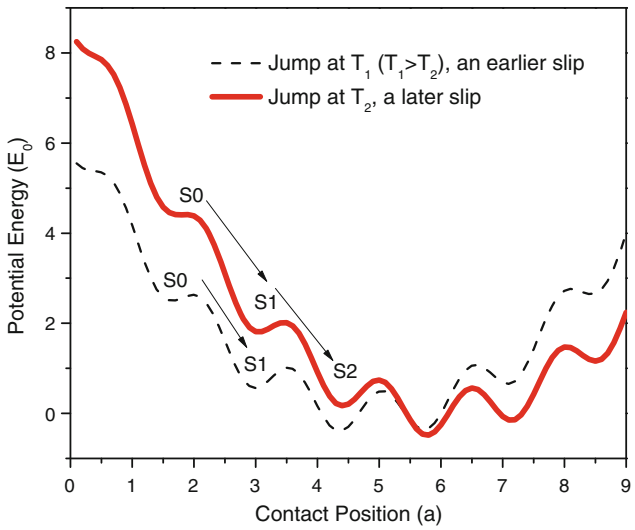

Fig. 9 Potential energy landscape as a function of contact position from a 1D Tomlinson model. The *dash* and *solid curves* correspond to an earlier time (smaller support position) and a later time (larger support position), respectively. a and E_0 are the periodicity and amplitude of the corrugation potential, respectively. At temperature T_1 ($T_1 > T_2$), slips can occur earlier than those at T_2 by overcoming barriers via a stronger thermal activation. See text for details

model is expected to be more robust against the specific value of the damping parameter.

In the following, we consider the commensurate system with a very soft cantilever $K_1 = 2.3$ N/m, corresponding to $\eta = 108$. In this regime, about 20 minima are available to the system at any given time. Simulations are run at a support sliding velocity of 2 m/s and temperatures between 0 and 400 K. We first investigate the effect of temperature on the number of slips. Friction traces and slip lengths at 0, 200, and 400 K are shown in Fig. 7. The corresponding averaged slip length and mean friction are reported in Fig. 8. The results show that only double slips are observed at $T = 0$ K. Upon raising the temperature, the occurrence of single slips increases significantly, resulting in a decrease of the average slip length. This trend reverses around 150 K because increasingly long slips (e.g., triple and quadruple) start to occur, leading to a turnover of the average slip length.

The observed trend can be rationalized as follows (c.f. Fig. 9): at $T = 0$ K, slip occurs when a minimum is completely de-stabilized by the cantilever's elastic potential energy. At this point, the amount of deformation energy stored in the tip and cantilever is maximal and the energy barriers for subsequent slips downhill in energy are at their minimum. When slip occurs, this potential energy is converted into kinetic energy that can fuel multiple consecutive slips insofar as they occur before the coherent motion of the tip is damped. In the present case, this translates into the occurrence of double slips. At finite temperature, slips are thermally activated before the instability points. This means that the potential energy stored in the system at the occurrence of slip is reduced and the energy barriers that need to be overcome to complete multiple slips are larger than in the athermal case. These two effects should lead to a decrease in the probability of multiple slips, and hence of the average slip length, in agreement with our simulation results below $T = 150$ K. As the temperature is increased further, an opposite effect comes into play. The velocity of the system as it crosses the saddle plane associated with slip is canonically distributed. Higher temperature means larger average velocities along the reaction coordinate, and hence an additional source of energy that can be tapped into to complete multiple slips. This contribution becomes more and more dominant as the temperature increases [33], leading to an increase of the average slip length around $T = 150$ K.

The monotonic decrease of friction with temperature we observe is consistent with some recent model and experimental results ([11] and [15], respectively) but inconsistent with other model and experimental results that predict a friction peak at finite temperature ([10] and [14], respectively). The friction peak is described as a result of the competition between increasing friction due to bond formation in the contact interface and decreasing friction due to thermal excitation [34]. One possible explanation for the discrepancy is that the characteristics of metallic bonding are different from those of covalent or ionic bonding. However, we are unable to quantitatively evaluate this hypothesis because there is no clear definition of a metallic bond (metallic bonding is a collective phenomenon including the interactions between nuclei as well as the embedding energy due to the free electron sea). The few

experimental studies of atomic friction on metal surfaces that have been reported (Au [35] and Pt [36]) do not describe temperature dependance and so direct comparison of our results is not possible at this time.

We also investigate the effect of scanning velocity on transitions between single and multiple slips as shown in Figs. 10 and 11. Since velocity and temperature are fundamentally related, the mechanisms through which velocity affects stick-slip are similar to those discussed in the previous section: at high velocity, slips occur close to the instability point and the potential energy stored in the cantilever at the onset of slip is large, leading to a higher proportion of multiple slips. As the velocity decreases, slips occur earlier and the average slip length correspondingly decreases. Here, there is no thermally induced turnover, so the slip length decreases monotonously with decreasing velocity. In this specific case, the slip length decreases to the point where only single slips are observed, but in practice the efficiency of this multiple slip inhibition could be highly system dependent. Consistent with nearly all previous model- and experiment-based results (see for example [11–13]), we observe that friction increases monotonically with velocity.

As is illustrated in Fig. 7, multiple slips are accompanied by large drops in the friction force, which suggests that larger slip lengths will correspond to lower mean friction. While this statement is correct, the effect of multiple slips proved to be modest compared to the intrinsic temperature dependence of the friction. As shown in Fig. 8, a change in temperature from 0 to 400 K results in a reduction of friction by about 1.3 nN. In comparison, the decrease in friction due to the presence of multiple slips (as obtained by estimating the difference in mean friction measured from a multiple slip system and the mean friction

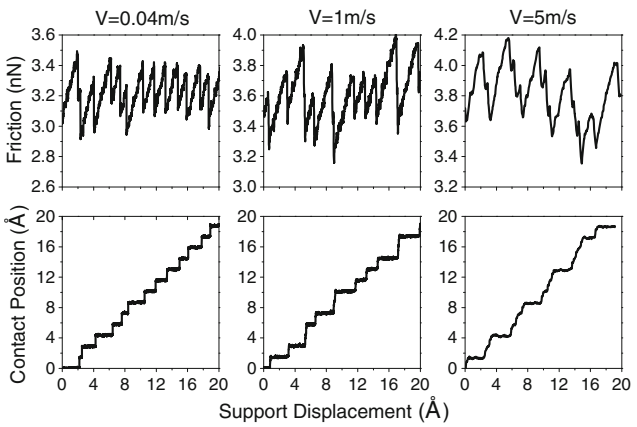

Fig. 10 The effect of velocity on multiple-slip: friction force (*top*) and contact position (*bottom*), as functions of support position for velocities of 0.4, 1.0, and 5.0 m/s. Larger jumps lengths at faster velocities indicate more multiple-slip

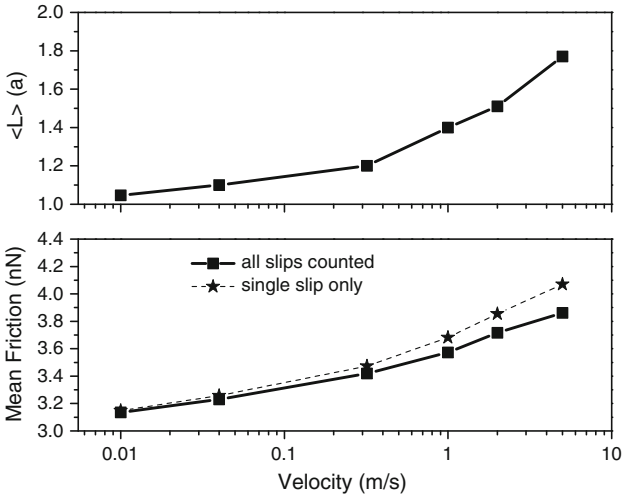

Fig. 11 Average slip length $\langle L \rangle$ and mean friction as a function of velocity. The *solid line* with *squares* is the measured average and the *dash line* with *stars* is the predicted average if only single slips would have occurred. a is the length of a single slip

that would have arisen if single slips alone would have occurred) ranges between about 0.16 and 0.08 nN. Similarly, when velocity is varied (c.f. Fig. 11) the change in friction due to multiple slips is not the dominant contribution to the velocity dependence of friction. We however note that, for stiffer cantilevers, the dependence of the mean friction on the average slip length will be more pronounced and might modify the balance between the different contributions.

4 Conclusion

In this study, we have introduced compliance into a fully atomistic simulation of a metallic AFM tip/substrate system to investigate its effect on atomic friction. Compliance is shown to play a critical role in determining not only the mean friction, but also transitions between friction regimes. The energy landscape with different compliance obtained from molecular statics calculation shows that theoretical prediction of the critical values for η are applicable for the fully atomistic system considered here. This is found to approximately hold even for complex transition coordinates that are not colinear with the scanning direction. Although the theoretical parameters predict possible transitions, molecular dynamics simulation reveals that dynamic effects including scanning velocity and temperature ultimately determine the slip mode. Simulations show that the temperature-induced variation of the slip length is, in contrast with the velocity dependence, non-monotonic. While the relative importance of variations in the slip modes proved to be small compared to that of velocity and temperature for our system, we expect that less compliant

systems could be significantly affected, opening the door to an enhanced control of friction at the nanoscale.

Acknowledgments We are grateful for the contributions of Jianguo Wu, Dr. Qunyang Li and Dr. Robert Carpick and to the National Science Foundation for its support via award CMMI- 0758604. Work at Los Alamos National Laboratory (LANL) was supported by the United States Department of Energy (U.S. DOE) Office of Basic Energy Sciences, Materials Sciences and Engineering Division, and by the LANL Laboratory Directed Research and Development Program. LANL is operated by Los Alamos National Security, LLC, for the National Nuclear Security Administration of the U.S. DOE under Contract No. DE-AC52-06NA25396.

References

1. Dienwiebel, M., Verhoeven, G.S., Pradeep, N., Frenken, J.W.: Superlubricity of graphite. Phys. Rev. Lett. **92**, 126101 (2004)
2. Socoliuc, A., Bennewitz, R., Gnecco, E., Meyer, E.: Transition from stick-slip to continuous sliding in atomic friction: entering a new regime of ultralow friction. Phys. Rev. Lett. **92**, 134301 (2004)
3. Krylov, S.Y., Jinesh, K.B., Valk, H., Dienwiebel, M., Frenken, J.W.M.: Thermally induced suppression of friction at the atomic scale. Phys. Rev. Lett. **71**, 065101 (2005)
4. Socoliuc, A., Gnecco, E., Maier, S., Pfeiffer, O., Baratoff, A., Bennewitz, R., Meyer, E.: Atomic-scale control of friction by actuation of nanometer-sized contacts. Science **313**, 207 (2006)
5. Mate, C.M., McClelland, G.M., Erlandsson, R., Chiang, S.: Atomic-scale friction of a tungsten tip on a graphite surface. Phys. Rev. Lett. **59**, 1942–1945 (1987)
6. Zhong, W., Tománek, D.: First-principles theory of atomic-scale friction. Phys. Rev. Lett. **64**, 3054–3057 (1990)
7. Medyanik, S.N., Liu, W.K., Sung, I.-H., Carpick, R.W.: Predictions and observations of multiple slip modes in atomic-scale friction. Phys. Rev. Lett. **97**, 136106 (2006)
8. Perez, D., Dong, Y., Martini, A., Voter, A.F.: Rate theory description of atomic stick-slip friction. Phys. Rev. B **81**, 245415 (2010)
9. Conley, W.G., Krousgrill, C.M., Raman, A.: Stick-slip motions in the friction force microscope: effects of tip compliance. Tribol. Lett. **29**, 23–32 (2008)
10. Tshiprut, Z., Zelner, S., Urbakh, M.: Temperature-induced enhancement of nanoscale friction. Phys. Rev. Lett. **102**, 136102 (2009)
11. Sang, Y., Dube, M., Grant, M.: Thermal effects on atomic friction. Phys. Rev. Lett. **87**, 174301 (2001)
12. Gnecco, E., Bennewitz, R., Loppacher, C., Bammerli, M., Meyer, E., Guntherodt, H.-J.: Velocity dependence of atomic friction. Phys. Rev. Lett. **84**, 1172–1174 (2000)
13. Riedo, E., Gnecco, E., Bennewitz, R., Meyer, E., Brune, H.: Interaction potential and hopping dynamics governing sliding friction. Phys. Rev. Lett. **91**, 084502 (2003)
14. Shirmeisen, A., Jasen, L., Hölscher, H., Fuchs, H.: Temperature dependence of point contact friction on silicon. Appl. Phys. Lett. **88**, 123108 (2006)
15. Zhao, X., Phillpot, S.R., Sawyer, W., Sinnott, S.B., Perry, S.S.: Temperature dependence of point contact friction on silicon. Phys. Rev. Lett. **102**, 186102 (2008)
16. Roth, R., Glatzel, T., Steiner, P., Gnecco, E., Baratoff, A., Meyer, E.: Multiple slips in atomic-scale friction: an indicator for the lateral contact damping. Tribol. Lett. **39**, 63–69 (2010)
17. Nakamura, J., Wakunami, S., Natori, A.: Double-slip mechanism in atomic-scale friction: Tomlinson model at finite temperatures. Phys. Rev. B **72**, 235415 (2005)
18. Voter, A.F.: Embedded atom method potentials for seven FCC metals: Ni, Pd, Pt, Cu, Ag, Au, and Al. Los Alamos Unclassifed Technical Report LA-UR-93-3901 (1993)
19. Martini, A., Dong, Y., Perez, D., Voter, A.F.: Low-speed atomistic simulation of stick slip friction using parallel replica dynamics. Tribol. Lett. **36**, 63–68 (2009)
20. Voter, A.F.: Parallel replica method for dynamics of infrequent events. Phys. Rev. B **57**, 13985–13988 (1998)
21. Liu, D.C., Nocedal, J.: On the limited memory BFGS method for large scale optimization. Math. Program. **45**, 503 (1989)
22. E, W., Ren, W., Vanden-Eijnden, E.: String method for the study of rare events. Phys. Rev. B **66**, 052301 (2002)
23. Krylov, S., Dijksman, J.A., van Loo, W.A., Frenken, J.M.: Stick-slip motion in spite of a slippery contact: do we get what we see in atomic friction?. Phys. Rev. Lett. **97**, 166103 (2006)
24. Krylov, S.Y., Frenken, J.W.M.: Thermal contact delocalization in atomic scale friction: a multitude of friction regimes. New. J. Phys. **9**, 398 (2007)
25. Bennewitz, R., Gyalog, T., Gussisberg, M., Meyer, E., Guntherodt, H.-J.: Atomic-scale stick-slip processes on Cu(111). Phys. Rev. B **60**, 301–304 (1999)
26. Carpick, R., Ogletree, D.F., Salmeron, M.: Lateral stiffness: a new nanomechanical measurement for the determination of shear strengths with friction force microscopy. Appl. Phys. Lett. **70**, 1 (1997)
27. Lantz, M.A., Oshea, S.J., Hoole, A.C.F., Welland, M.E.: Lateral stiffness of the tip and tip-sample contact in frictional force microcopy. Appl. Phys. Lett. **70**, 8 (1997)
28. Johnson, K.L., Woodhouse, J.: Stick-slip motion in the atomic force microscope. Tribol. Lett. **5**, 155 (1998)
29. Kim, W.K., Falk, M.L.: Atomic-scale simulations on the sliding of incommensurate surfaces: the breakdown of superlubricity. Phys. Rev. B **80**, 235428 (2009)
30. Hirano, M., Shinjo, K.: Atomistic locking and friction. Phys. Rev. B **41**, 11837 (1990)
31. Sørensen, M.R., Jacobsen, K.W., Stoltze, P.: Simulations of atomic-scale sliding friction. Phys. Rev. B **53**, 2101–2113 (1996)
32. Maier, S., Sang, Y., Filleter, T., Grant, M., Bennewitz, R., Gnecco, E., Meyer, E.: Fluctuations and jump dynamics in atomic friction experiments. Phys. Rev. B **72**, 245418 (2005)
33. Voter, A.F., Doll, J.D.: Dynamical corrections to transition state theory for multistate systems: surface self-diffusion in the rare-event regime. J. Chem. Phys. **82**, 80–92 (1985)
34. Barel, I., Urbakh, M., Jansen, L., Schirmeisen, A.: Multibond dynamics of nanoscale friction: the role of temperature. Phys. Rev. Lett. **104**, 066104 (2010)
35. Gosvami, N.N., Filleter, T., Egberts, P., Bennewitz, R.: Microscopic Friction Studies on Metal Surfaces. Tribol. Lett **39**, 19–24 (2010)
36. Enachescu, M., Carpick, R.W., Ogletree, D.F., Salmeron, M.: The role of contaminants in the variation of adhesion, friction, and electrical conduction properties of carbide-coated scanning probe tips and Pt(111) in ultrahigh vacuum. J. Appl. Phys. **95**, 7694 (2004)